Aeronautical Ground Lighting System Study: Field Measurements and Simulations

D. Vidal[1], Ll. Monjo[2], L. Sainz[2*]

[1] A.A.S.A. Airport of Reus, Reus, 43206, Spain
[2] Department of Electrical Engineering, ETSEIB-UPC, Av. Diagonal 647, Barcelona 08028, Spain
[*] sainz@ee.upc.edu

Abstract: Aeronautical ground lighting (AGL) systems are single-phase series circuits where constant current regulators supply transformers and luminaires. These systems provide visual reference to aircraft during airport operations. There is a lack of AGL system models and measurements in the literature to study AGL system behavior and predict their response to electrical events and future technological changes. The paper contributes to AGL system modeling with an equivalent circuit useful to study AGL system concerns by Matlab/Simulink simulations. It also presents field measurements taken at Reus airport (Catalonia, Spain) for the validation of the proposed model and understanding of AGL system behavior in the event of luminaire failure.

1. Introduction

Aeronautical ground lighting (AGL) systems provide visual cues to help aircraft pilots during approach, landing and taxiing [1]. These systems are single-phase series circuits where constant current regulators (CCRs) supply luminaires through transformers with voltages up to 5 kV (see Fig. 1) [1] –[9]. CCRs are variable voltage sources, [10], [11], which provide an adjustable rms current according to luminaire brightness requirements and ensure circuit continuity, even in case of luminaire failure [4], [6], [7]. Their standard power ratings are 4, 7.5, 10, 15, 20, 25, 30, 50 and 70 kVA with a typical current rating of 6.6 A. Luminaires are visual aids for pilots whose number ranges from 10 up to 300 in small and large AGL systems, respectively. Their pattern, intensity (high and low), color and direction of light emission

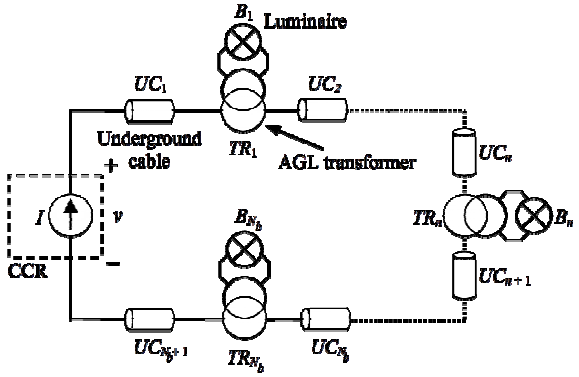

Fig. 1. AGL system

depend on AGL system requirements [1], [2], [4], [12]. They provide five discrete brightness steps according to rms current values (6.6, 5.2, 4.1, 3.4 and 2.8 A or 20.0, 15.8, 12.4, 10.3 and 8.5 A) [1], [2], [4]. AGL system luminaires are usually halogen lamps. However, they are currently being replaced by LED lamps according to energy saving policies [13]. AGL transformers separate CCRs and luminaires into primary and secondary circuits. They ensure series circuit continuity even in case of luminaire failure and isolate luminaires from the high operating voltage of the primary circuit. In the event of luminaire failure, the transformers maintain circuit continuity but work in saturation, modifying CCR operating conditions and reducing AGL system power quality [7], [14], [15].

AGL systems require expensive maintenance and conservation work and pose power quality concerns mainly derived from electrical events (e.g., luminaire failure) [5], [7], [8], electrical safety issues (e.g., cable insulation failure and lightning strikes) [7], [14], [16], system control (e.g., lamp monitoring) [3], [4], [5], [12] and future technological changes (e.g., changes in luminaire technology) [13]. AGL system modeling is required to simulate and accurately predict system response to the above electrical events. Several works on this topic (e.g., modeling of CCRs [4], [6], cables [5], [7], [16], transformers [5], [15] and luminaires [5], [7], [13]) are currently available. In [4] and [6], different CCR technologies are described, measurements of CCR voltage and current waveforms are plotted and CCR modeling is briefly discussed. In [5], AGL system architecture is presented and AGL system components are analyzed in the laboratory and modeled with an approximate circuit using SPICE to build a power-link model and examine a power-line communication method for controlling and monitoring luminaires (e.g., for detection and location of failed luminaires). In [7], a simple model of the AGL system equivalent circuit is used to look at electrical safety issues during maintenance of AGL systems (particularly, in open-circuited secondary windings and faulty insulation between primary and secondary windings of AGL transformers). In [15], an AGL transformer model including transformer core saturation is presented and its parameters are estimated from laboratory measurements. The impact of failed luminaires on AGL systems due to transformer saturation is also pointed out. In [16], lighting interaction with AGL systems is analyzed using transmission line theory, ignoring lumped devices along the cable (i.e., CCRs and transformers) and neglecting nonlinear phenomena. It must be noted that the above works present simple models of AGL systems or models of only one of their components to study AGL system behavior under specific conditions. However, there is no contribution in AGL system modeling to accurately simulate AGL system response under different operating conditions from a complete AGL system equivalent circuit. Field measurements in AGL systems are also necessary to study system response to electrical events but only a small number have been made due to the difficulty in accessing runways [5], [6], [8], [16].

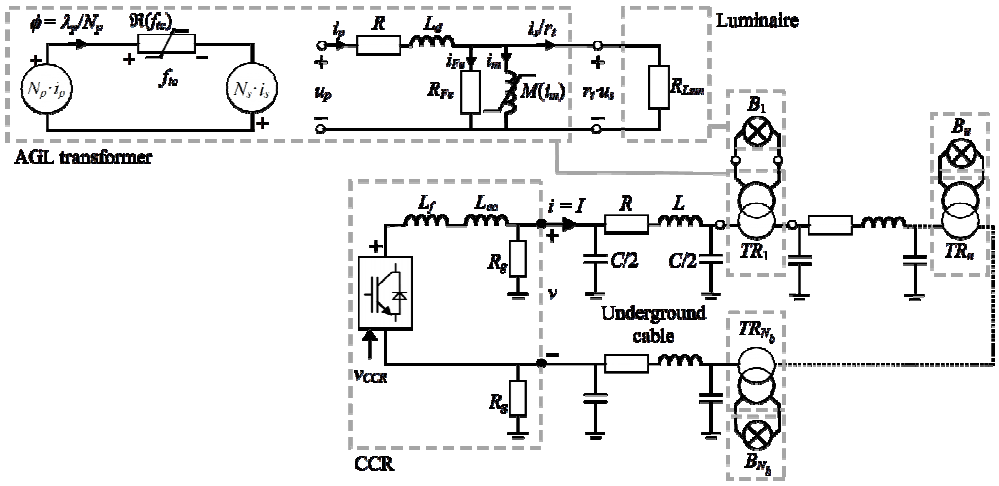

Fig. 2. Equivalent circuit of AGL systems

The paper presents an AGL system equivalent circuit which considers CCR control, underground cable concentrated parameters and transformer saturation. This circuit allows Matlab/Simulink simulations [17] to be performed and covers the lack of an AGL system general model in the literature for accurately analysing most of the above discussed electrical events. Moreover, field measurements in two AGL systems with 4 and 68 luminaires taken in different operating conditions at Reus airport are reported to validate the accuracy of the model and provide insights into the impact of failed luminaires on AGL systems.

2. AGL system equivalent circuit

AGL systems are series circuits of copper insulated underground cables where CCRs supply luminaires through transformers with adjustable rms current. Fig. 1 shows the basic circuit of these systems. The equivalent circuit in Fig. 2, obtained from the AGL component models presented in the following subsections, is proposed for AGL system modelling. This circuit can be implemented in Matlab/Simulink to predict AGL system behavior and can be used to study most AGL systems under several operating conditions [3]–[8], [14], [16].

2.1. CCR model

Constant current regulators receive the AC input supply and provide an adjustable rms current I according to requirements of five discrete brightness steps [1], [2], [4], [6]. Until a few years ago, CCRs used phase control with ferro-resonant transformers to provide adjustable output current. Now, they use pulse width modulated (PWM) converters based on insulated gate bipolar transistors (IGBTs) because

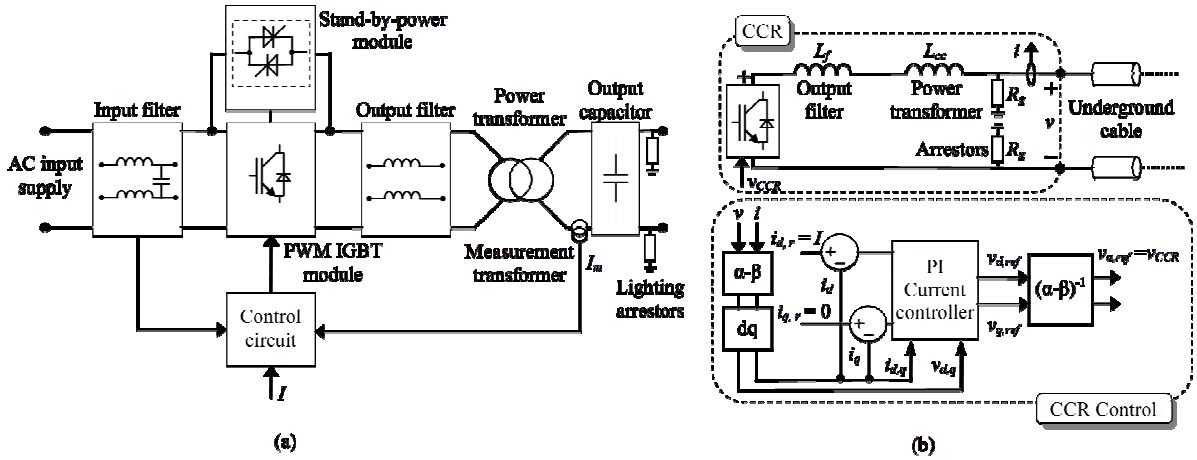

Fig. 3. Equivalent circuit of AGL constant current regulator
a Block diagram
b CCR model

they are more efficient than the former [4], [6]. Fig. 3(a) shows the typical block diagram of a CCR that uses a PWM IGBT converter to regulate current [6], [9]. It mainly includes an input filter to comply with electromagnetic compatibility (EMC) levels and mitigate harmonics generated by the power module, a PWM IGBT power module to generate sine output voltage waveforms, a control circuit of the PWM IGBT power module, a power transformer to increase the output voltage and isolate the CCR from the series circuit and a feedback transformer coupled to the secondary winding of the power transformer to provide the current feedback signal to the controller. Regulators may further include a stand-by-power module which is automatically connected in case of main power module failure, an output filter consisting of an inductance which filters the PWM carrier frequency and an output capacitor to compensate power transformer reactive power and mitigate harmonics. CCRs are also usually fitted with earth fault detectors and lighting arrestors installed at their output terminals and connected to an earth ground electrode [7], [9]. The control circuit provides the IGBTs with PWM trigger signals (obtained from a 5 – 8 kHz carrier and a line frequency modulation sine wave) and adjusts their duty cycle based on the typical *dq* synchronous reference frame PI technology [10], [11]. This allows the comparison between rms values of the actual current measurement I_m and the reference current I, and fast and automatic stabilization of the output current in the presence of disturbance (e.g., luminaire failure) to meet the desired luminaire brightness values. According to Fig. 3(b), CCRs are modelled as a controlled sinusoidal voltage source in series with the short-circuit inductance of the power transformer. The ground connected resistances R_g ($\approx$ MΩ) model the earth fault detectors and lighting arrestors installed at the CCR output terminals. The control circuit provides the IGBTs with PWM trigger signals (obtained from a 5 – 8 kHz carrier and a line frequency modulation sine wave) and adjusts their duty cycle based on the typical *dq* synchronous reference frame PI

technology [10], [11]. Thus, the rms value V_{CCR} of the sinusoidal voltage source is imposed by a PI controller in order to compensate for the error between the rms value I_m of the actual current i and the reference current value I. The value of the short-circuit inductance L_{cc} can be determined from voltage and current measurements at the primary and secondary windings of the CCR power transformer.

2.2. Underground cable model

AGL systems are single-phase series circuits of screened single-core insulated cables with cooper cross sections ranging from 6 mm^2 to 8 mm^2 [1], [2], [5]. The cables are usually installed in an underground duct bank or directly buried [7]. Since length of AGL system cables is typically smaller than 10 km and the shortest wavelength used in common AGL system operating conditions with frequencies below 2.5 kHz is approximately greater than 40 km, a π-equivalent circuit based on the concentrated parameter model is proposed (see Fig. 2). The line conductance is neglected and the concentrated parameters R, L and C are obtained from the distributed parameters R_x, L_x and C_x and length D of the cable,

$$R = R_x \cdot D \qquad L = L_x \cdot D \qquad C = C_x \cdot D. \tag{1}$$

Distributed parameter data values are obtained from the cable type and datasheet of the cable manufacturer.

2.3. AGL transformer model

AGL transformers are single-phase transformers generally consisting of a rectangular magnetic core and separate primary and secondary windings. Their power rating ranges from 30 to 500 W and their current ratio is generally 6.6/6.6 A (i.e., the winding turn ratio r_t is equal to 1). The AGL transformer model in [15], which considers transformer core saturation, is used in the paper. This model is shown in Fig. 2, where R and L_d are the winding resistance and constant leakage inductance, R_{Fe} is the core loss resistance, $M(i_m)$ is the core non-linear magnetizing inductance, which depends on the magnetizing current i_m, and $\Re(f_{tc})$ is the core non-linear reluctance, which depends on the magnetic potential f_{tc} in the transformer core.

According to Fig. 2, the electric relations of transformers are

$$\begin{aligned} &u_p = \left(R + L_d \frac{d}{dt}\right) i_p + r_t \cdot u_s \qquad u_s = \frac{1}{r_t} \frac{d(M(i_m) \cdot i_m)}{dt} \qquad 0 = R_{Fe} \cdot i_{Fe} - \frac{d(M(i_m) \cdot i_m)}{dt} \\ &i_m = i_p - i_s / r_t - i_{Fe}, \end{aligned} \tag{2}$$

and the magnetic flux and current relations are

$$\begin{aligned} N_p \cdot i_p - N_s \cdot i_s &= f_{tc} \\ f_{tc} &= \Re(f_{tc}) \cdot \phi \end{aligned} \quad \Rightarrow \quad i_p - \frac{i_s}{r_t} = \frac{\Re(f_{tc})}{N_p} \cdot \frac{\lambda_p}{N_p} \quad \Rightarrow \quad \lambda_p \approx N_p^2 \cdot \Re^{-1}(f_{tc}) \cdot i_m = M(i_m) \cdot i_m, \tag{3}$$

where $r_t = N_p/N_s$ is the winding turn ratio, N_p and N_s are the primary and secondary winding turns and $\lambda_p = M(i_m) \cdot i_m$ is the core magnetic flux across the primary winding. Note that the current flowing through the core loss resistance is much smaller than the primary and secondary currents and is neglected in (3), i.e., $i_m \approx i_p - i_s/r_t$. The following functional relationship is used to characterize the core saturation curve $M(i_m)$ by means of an anhysteretic magnetization curve [15]:

$$M\left(i_m\right) = \frac{M_1}{\left(1 + (i_m/i_0)^p\right)^{1/p}} + M_2, \tag{4}$$

where M_1, M_2, p and i_0 are experimental parameters allowing the fitting of the above reluctance function to the core saturation curve. The equivalent circuit parameters R, L_d, R_{Fe} and the core magnetizing inductance $M(i_m)$ of the transformer model are obtained from voltage and current laboratory measurements [15].

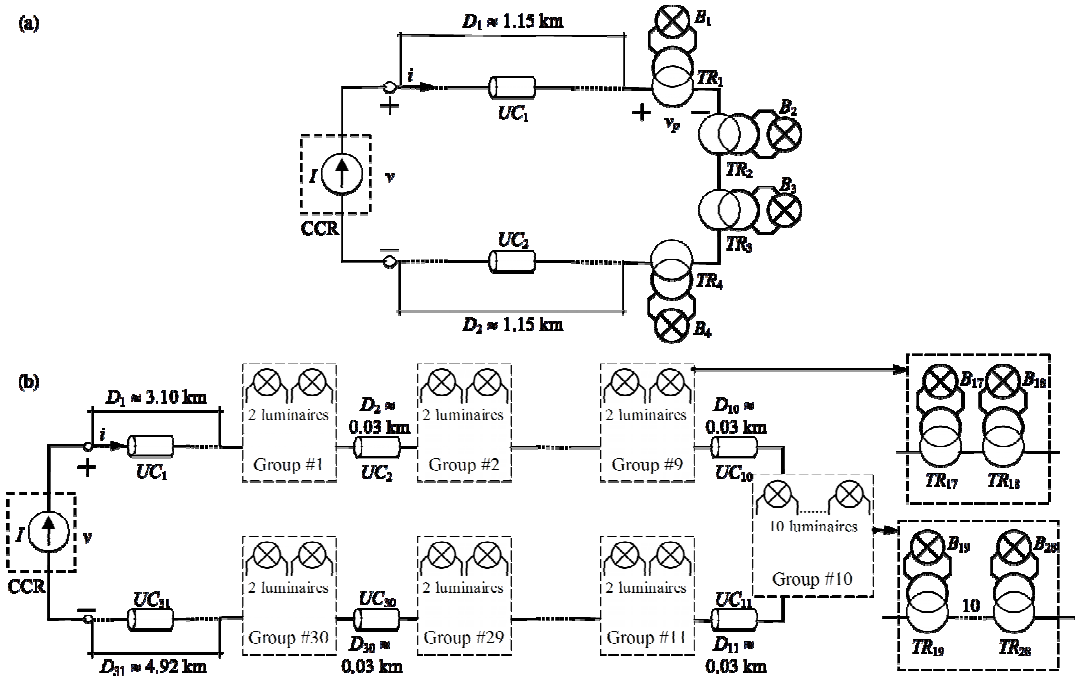

Fig. 4. *AGL system tests*
a 4 luminaire AGLsystem
b 68 luminaire AGLsystem

2.4. Luminaire model

AGL system luminaires are usually halogen lamps which are modelled as a resistance [5], [7]. It was experimentally verified that their value can be accurately calculated from the luminaire active power and the current rating of the AGL system highest brightness step (i.e., $R_{Lum} = P_{Lum}/I_{hs}^2$ with $I_{hs} = 6.6$ A).

3. AGL system measurements and simulations

Field measurements were conducted on two circuits with 4 and 68 luminaires (see Fig. 4) under different operating conditions at Reus airport in order to study AGL system behavior. Measurements were made with a SIGLENT SDS1102CML digital scope and numerically processed in a computer. Additionally, Matlab/Simulink (v2012b) simulations on Intel i3 CPU 3.2 GHz with 4 GB of RAM were performed to validate the equivalent circuit in Fig. 2. Modelization of components was based on Power System Blockset. The simulations were configured with the variable step solver ode23 using a trapezoidal rule. The maximum value of the step was set at 0.25 μs. The parameters in Table 1 (obtained from manufacturer datasheets and laboratory and field measurements) were used in the simulations.

3.1. AGL system measurements

3.1.1. AGL system with 4 luminaires: Fig. 4(a) illustrates the 2.3 km AGL system circuit corresponding to the airport runway stop bar with a 2.5 kVA CCR supplying 4 luminaires of 8W connected through 45 W 6.6/6.6 A 50 Hz transformers one after the other. Measurements were performed for the typical five

Table 1 AGL system parameters

	Parameters	4 luminaire system	68 luminaire system
CCR	Model	ADB CRE 2.5 kVA	OCEM UR2000-2100 25 kVA
	L_{cc} (mH)	2.39	250
Underground cable	R_x (Ω/km)	3.98	3.98
	L_x (mH/km)	0.547	0.547
	C_x (μF/km)	0.126	0.126
6.6/6.6 A 50 Hz AGL transformer [15]	P (W)	45	150
	R (Ω)	0.187	0.281
	L_d (mH)	0.370	1.19
	M_1 (mH)	176.5	693.8
	M_2 (mH)	1.10	1.80
	p (pu)	1.11	0.906
	i_0 (A)	0.347	0.286
Luminaire	P (W)	48	150

brightness steps and with all the luminaires on and one, two, three and four failed luminaires. However, for the sake of space, only measurement results with the current rating of the highest brightness step and zero, one and three failed luminaires (i.e., 4, 3 and 1 luminaires on, respectively) are shown in Fig. 5. Fig. 5(a) plots the measured voltage v and current i at the CCR output terminals (grey continuous lines) and Fig. 5(b) shows their harmonic spectra (light grey bars). These harmonic spectra are analyzed with the individual and total harmonic distortions (*HD* and *THD*),

$$HD_x = \frac{X_k}{X_1} \qquad THDx = \frac{\sqrt{\sum_{k>1} X_k^2}}{X_1} \qquad (x = v, i), \tag{5}$$

where X_1 and X_k are the rms values of the fundamental and harmonics, respectively.

3.1.2. AGL system with 68 luminaires: Fig. 4(b) illustrates the 8.89 km AGL system circuit corresponding to the approach lighting system with a 25 kVA CCR supplying 68 luminaires of 150 W connected through 150 W 6.6/6.6 A 50 Hz transformers. Measurements were performed for the typical five brightness steps and with all the luminaires on and one, two, four, six, eight and ten failed luminaires. However, for sake of

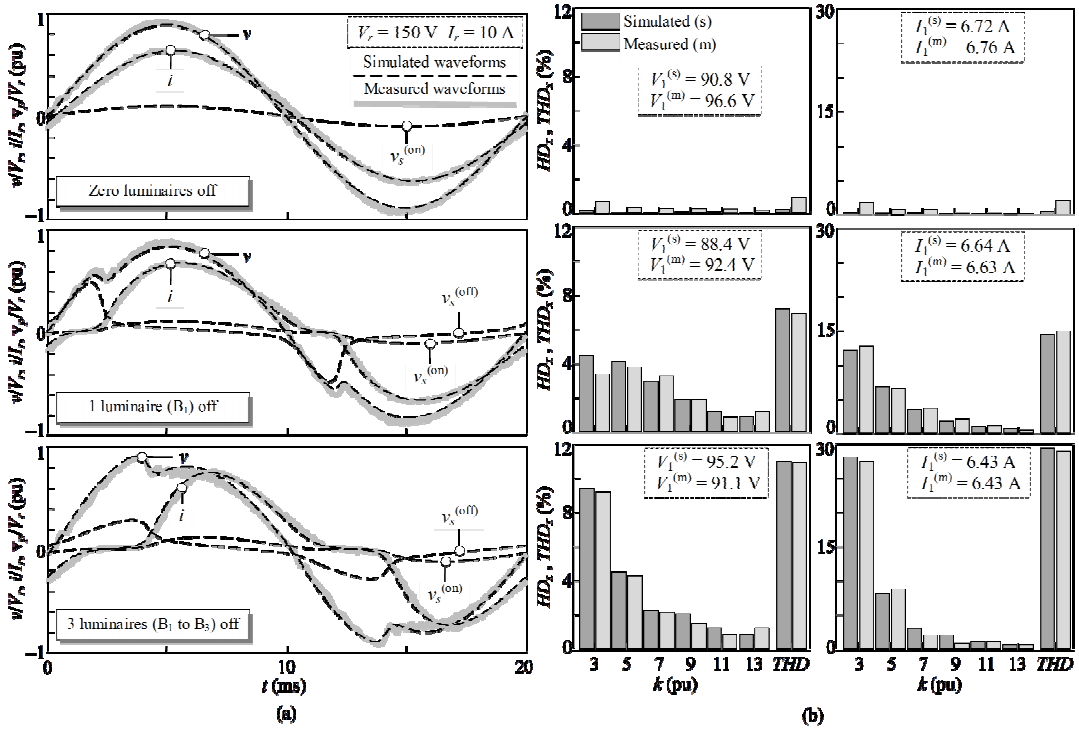

Fig. 5. *Results of the 4 luminaire AGL system*
a Voltage and current waveforms
b Voltage and current harmonic spectra

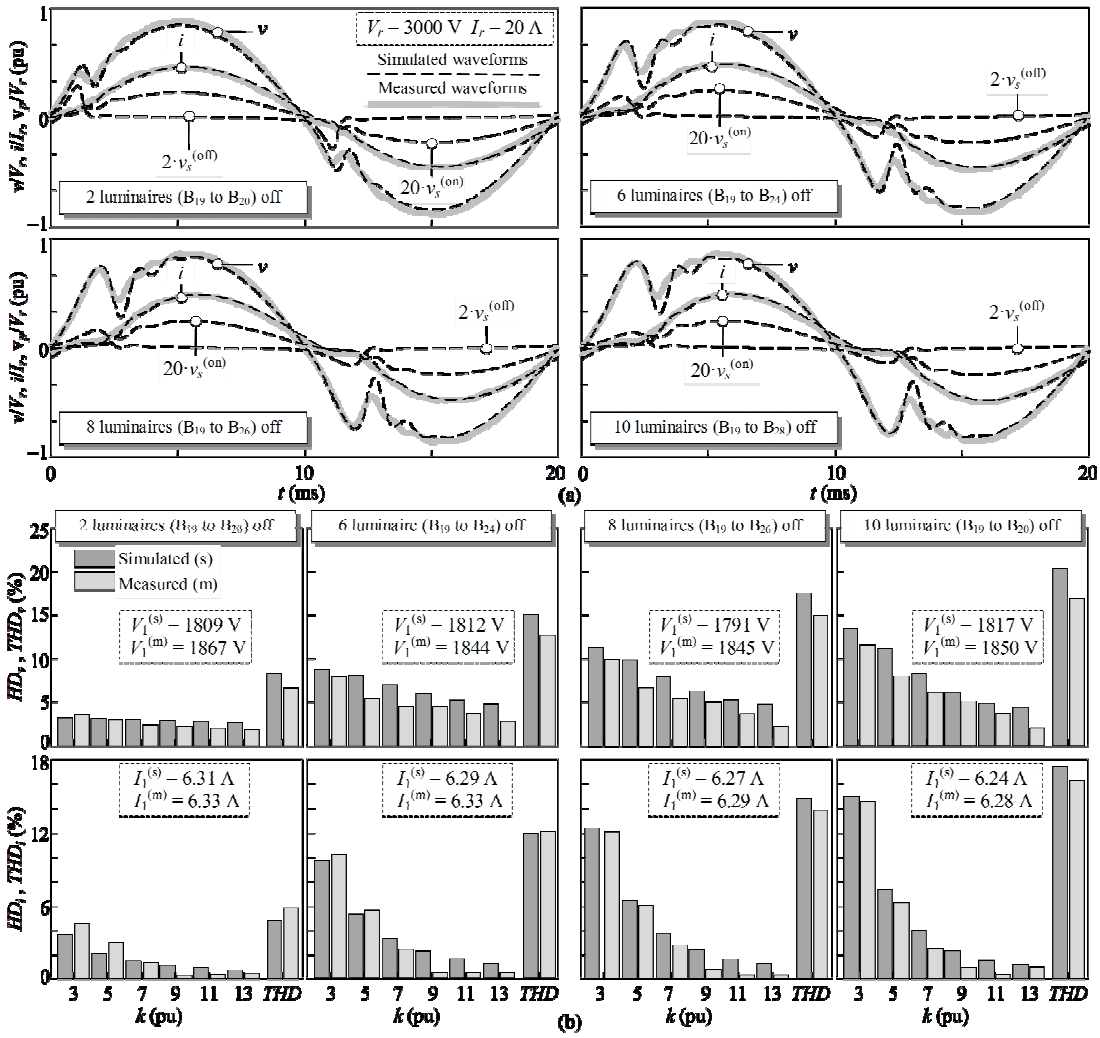

Fig. 6. *Results of the 68 luminaire AGL system*
a Voltage and current waveforms
b Voltage and current harmonic spectra

space, only measurements with the current rating of the highest brightness step and two, six, eight and ten failed luminaires (i.e., 66, 62, 60 and 58 luminaires on, respectively) are shown in Fig. 6. The test voltage and current with all the luminaires on were 1959 V and 6.16 A 50 Hz sinusoidal waveforms, respectively. Fig. 6(a) plots the measured voltage *v* and current *i* at the CCR output terminals (grey continuous lines) and Fig. 6(b) shows their harmonic spectra (light grey bars).

3.1.3. Test result notes: The following observations can be made from the measurements in Fig. 5 and Fig. 6:

- In the event of luminaire failure, the transformers maintain circuit continuity but work in

saturation because they operate in open circuit at series circuit rated current. This must be considered in AGL system studies because saturation results in harmonic currents in the AGL system, modifying CCR operating conditions and reducing AGL system power quality. It is concluded from the test results that luminaire failure can lead (particularly, in small AGL systems) to total harmonic distortions of the consumed current above 20 %.

- A large number of failed luminaires leads to a sharp consumed current waveform and increases harmonic current and voltage distortion above Standard limits (e.g., IEC 6100-3-2 [18] and EN 5160 [19] limits, respectively). This phenomenon may cause power quality problems such as malfunction of AGL system electronic equipment (e.g., CCRs and LED luminaires, which are currently replacing halogen luminaires) and insulation stress of AGL transformers [7].
- Although harmonic current emissions in the 68 luminaire circuit are much lower than in the 4 luminaire circuit, harmonic voltage distortion is similar in both circuits. This is revealed from the 9th to 13th harmonic in Fig. 5(b) and Fig. 6(b) because the 68 luminaire circuit voltage distortion is high compared to the current distortion. The reason for this could be parallel resonance occurring in this circuit. This phenomenon can arise in AGL systems because they have both inductive CCR and capacitive cable characteristics. Harmonic current emissions of AGL saturated transformers are amplified around resonance frequencies in case of luminaire failure, leading to a possible increase in voltage distortion, and thus a reduction in power quality.

3.2. AGL system simulations

Figs. 5 and 6 also plot the simulated voltage v and current i at the CCR output terminals (black dashed lines) and show their harmonic spectra (dark grey bars). Comparison between these results and the field measurements illustrates the accuracy of the proposed equivalent circuit. The simulated voltage waveforms at the secondary windings of the AGL transformers with luminaires on and off ($v_s^{(on)}$ and $v_s^{(off)}$, respectively) are also plotted to analyse voltage distribution in all the transformers in the event of luminaire failure (it was not possible to measure these voltages in the AGL systems). The following observations can be made from the simulation results in Figs. 5 and 6:

- Simulations with the proposed equivalent circuit are useful for predicting AGL system response to luminaire failure accurately. In general, this circuit could be used to study other electrical events and future technological changes and analyse power quality and electrical safety issues (e.g., harmonic penetration studies, resonance phenomenon analysis, failed luminaire locations, steady state short-circuit research [7]).

- Simulations show that AGL transformers of failed luminaires withstand high secondary voltage peaks at primary current zero crossings. The voltage values of these peaks are greater than under normal operating conditions, and may therefore cause electrical safety problems in the secondary circuit of the AGL system [7]. Simulations also illustrate that this problem improves with the number of failed luminaires because the voltage drop is shared between their transformers. The proposed AGL equivalent circuit is a useful tool to analyse this phenomenon, which is difficult to measure in AGL systems.

4. Conclusion

The paper presents and analyses field measurements and simulations of luminaire failure in two AGL circuits at Reus airport. The following main conclusions can be drawn:

- Luminaire failure can lead to total voltage and current harmonic distortions above 5% and 10%, respectively, due to AGL transformer saturation. This could affect the correct operation of the AGL system and stress some of its components.
- The parallel resonance phenomenon can increase voltage distortions and reduce AGL system power quality.
- AGL transformers of failed luminaires withstand high secondary winding voltage peaks, which are an electrical safety concern during the replacement of luminaires.

Simulations were performed with a proposed AGL equivalent circuit which can be a powerful tool for developing more detailed work on the above and other concerns related to AGL system behavior in different conditions.

5. Acknowledgments

This research was carried out with the support of the Aena Aeropuertos S.A Reus Airport (Spain).

6. References

[1] 'Aerodrome design manual, Part 4: Visual aids', 4th Edition International Civil Aviation Organization, 2004

[2] 'Aerodromes, Volume I: Aerodrome design and operations', Annex 14 to the convention on International Civili Aviation, 4th Edition International Civil Aviation Organization, 2004

[3] Saraf, N., Salvi, R., Salunkhe, N., Sahasrabuddhe, R.: 'Airfield lamp monitoring & control systems'. Proc. Int. Conf. on Information, Communication and Embedded Systems (ICICES 2013), Febr. 2013, pp. 1141-1143

[4] Kevin, P. E.: 'Integration of aviation lighting system and computer controlled monitoring system'. Proc. IEEE Int. Conf. on Systems, Man and Cybernetics, Oct. 1996, pp. 1132-1137

[5] Granado, J., Chavez, J., Torralba, A., Oria Smith, A. C.: 'Modeling airfield lighting systems for narrowband power-line communications', IEEE Trans. on Power Delivery, 2014, **25**, (4), pp. 2399–2405

[6] Giardini, D. Galloway, J. H.: ' A single phase matrix down-converter for airport lighting regulation '. Proc. 34th IAS Annual Meeting Industry Applications, Oct. 2011, pp. 1153-1156

[7] Freschi, F., Mitolo, M., Tommasini, R.: 'Electrical safety of aeronautical ground lighting systems'. IEEE Trans. on Industry Applications, 2015, **51**, (3), pp. 2003–2008

[8] Sheng, C., Wenying, Y., Guoufu, Z.: 'Reliability analysis of airport lighting aid system based on light source failure'. Proc. 26th Int. Conf. on Electrical Contacts, May 2012, pp. 475-478

[9] OCEM AirfieldTechnology, 'Constant current regulators. New generation', EnergyTechnology

[10] Bahrani, B., Rufer, A., Kenzelmann, S., Lopes, L. A. C.: 'Vector control of single-phase voltage-source converters based on fictive-axis emulation', IEEE Trans. on Industry Applications, 2011, **47**, (2), pp. 831–840

[11] Teodorescu, R., Liserre, M., Rodríguez, P.: 'Grid converters for photovoltaic and wind power systems' (John Wiley and Sons publications, 1st edn. 2011)

[12] Smith, C. C.: 'Some aspects of airport lighting', Electronics and Power, 1970, **3**, pp. 85–89

[13] Wang, S., Wang, K., Chen, F., Zhao, S., Liu, S.: 'A novel LED lamp for the middle line of the taxiway of the airport'. Proc. 11th Int. Conf. on Electronic Packaging Technology & High Density Packaging (ICEPT-HDP), August 2010, pp. 1409-1411

[14] Bejleri, M., Rakov, V. A., Uman, M. A., Rambo, K. J., Mata, C. T., Fernandez, M. I.: 'Triggered lighting testing of an airport runway lighting system', IEEE Trans. on Electromagnetic Compatibility, 2004, **46**, (1), pp. 96–101

[15] Vidal, D., Monjo, Ll., Sainz, L., Pedra, J.: 'Model of aeronautical ground lighting system transformer', IET Electric Power Applications, 2015, **9**, (3), pp. 239–247

[16] Theethayi, N., Rakov, V. A., Thottappillil, R.: 'Responses of airport runway lighting system to direct lighting strikes: Comparisons of TLM predictions with experimental data', IEEE Trans. on Electromagnetic Compatibility, 2008, **50**, (3), pp. 660–668

[17] 'Matlab 7.9 (R2009b) and Simulink', The MathWorks, Natick, MA: 2009

[18] IEC-61000-3-2, Ed. 3: 'IEC Electromagnetic Compatibility (EMC), Part 3: Limits, Section 2: Limits for harmonics current emissions (equivalent input current < 16 A per phase)', 2005

[19] EN 50160: 'Voltage characteristics of electricity supplied by public electricity networks', 2011